

## Excitation of Roton in Helium II by Cold Neutrons

H. PALEVSKY,\* K. OTNES, AND K. E. LARSSON  
*A. B. Atomenergi, Stockholm, Sweden*

(Received May 29, 1958)

The nature of collective excitations in helium II has been investigated by means of the interaction of these excitations with cold neutrons. The experiment demonstrates the existence of excitations with long mean free path compared to their wavelength, confirming the theoretical ideas of Landau and Feynman. The dispersion relation for the excitations in the energy region of the "roton minimum" is directly measured and gives the following Landau parameters:  $\Delta=8.1\pm 0.4$  °K,  $P_0/\hbar=1.9\pm 0.03$  Å<sup>-1</sup> and  $\mu=0.16\pm 0.02$   $m_{\text{He}}$ .

### I. INTRODUCTION

THE theories of He II developed by Landau<sup>1</sup> and Feynman<sup>2</sup> lead to the conclusion that in helium below the  $\lambda$  point there exist localized excitations in the fluid, having mean free paths long compared to their wavelength. In general these excitations represent complicated motions of the fluid. However in certain limits the excitations can be described by simple models, *viz.*: phonons, characterized by a linear energy-momentum relationship  $E=cp$ , where  $c$  is the velocity of sound in helium II; and rotons, characterized by a quadratic energy-momentum relation of the form  $E=\Delta+(p-p_0)^2/2\mu$ , where  $\Delta$ ,  $p_0$ , and  $\mu$  are constants of the theory. Theoretical expressions for specific heat, second sound velocities, and superfluid concentration are obtained by integration over the energy spectrum of the excitations. Landau<sup>3</sup> showed that with  $\Delta=9.6$  °K,  $p_0/\hbar=1.95$  Å<sup>-1</sup>, and  $\mu=0.77$   $m_e$  a good fit to the existing experimental data was obtained.

Neutrons offer the possibility of investigating *directly* the energy-momentum relation of the excitations in condensed matter.<sup>4,5</sup> At the suggestion of Cohen and Feynman<sup>6</sup> such an experiment was undertaken in Stockholm.<sup>7</sup> These first measurements very strikingly demonstrated the existence of excitations with long mean free paths in He II. As the experiment progressed it was possible to determine point by point the energy-momentum relation in the region of the roton minimum energy  $\Delta$ . The present paper presents the experimental details of the first reported measurements together with the further measurements that have been made to date.

### II. PRINCIPLE OF METHOD

Neutrons provide a powerful tool for investigating the dynamical behavior of solids and liquids. Because of the neutron mass, neutrons with momenta comparable to momenta associated with excitations in condensed

matter have energies comparable or smaller than typical excitation energies in such matter. For this reason when the neutron interacts with a condensed system it transfers a *measurable* amount of its energy as well as its momentum.

In order to study the nature of the excitations in He II, an incident beam of "cold" neutrons (energy corresponding to a temperature  $\sim 50$  °K) is scattered by a sample of helium. The changes in neutron energy and momentum are measured and from these data the energy-momentum relation for the He II excitation is deduced. In general neutrons incident on a helium sample can lose or gain energy depending upon whether they produce or annihilate excitations in helium. However, with the sample near zero temperature, the cross section for production of excitations is much larger than for the annihilation process.<sup>6</sup> Therefore the former process is measured in the experiment.

The kinematics of the scattering are given by the conservation of energy and momentum

$$\frac{\hbar}{2m}(k_0^2 - k_f^2) = E(\kappa), \quad (1)$$

$$\hbar(\mathbf{k}_f - \mathbf{k}_0) = \boldsymbol{\kappa}, \quad (2)$$

where  $\hbar k_0^2/2m$  is the energy of the incident neutrons,  $\hbar k_f^2/2m$  is the energy of the scattered neutrons,  $E(\kappa)$  is the energy of the excitation in He II, and  $\boldsymbol{\kappa}$  is the momentum associated with the excitation  $E(\kappa)$ .

The above description of the scattering process has meaning if excitations in He II have a well-defined energy and momentum. For a normal liquid one knows that only in the limit of small momenta (wavelengths large compared to intermolecular spacings) can one properly speak of phonons in the above sense. One of the "strange" properties of He II, first postulated by Landau, is that excitations with wavelengths comparable to the mean separation of the liquid helium atoms have well-defined energy and momentum. Neutron measurements in principle determine whether the above condition exists. The spread in energies of the scattered neutrons as compared to the incident neutron energy spread, by the uncertainty principle, is a direct measure of the lifetime of the excitations in helium system.

\* Guest scientist on leave from Brookhaven National Laboratory, Upton, New York.

<sup>1</sup> L. Landau, J. Phys. (U.S.S.R.) **5**, 71 (1941).

<sup>2</sup> R. P. Feynman, Phys. Rev. **94**, 262 (1954).

<sup>3</sup> L. Landau, J. Phys. (U.S.S.R.) **11**, 91 (1947).

<sup>4</sup> G. Placzek and L. van Hove, Phys. Rev. **93**, 1207 (1954).

<sup>5</sup> Carter, Palevsky, and Hughes, Phys. Rev. **106**, 1168 (1957).

<sup>6</sup> M. Cohen and R. P. Feynman, Phys. Rev. **107**, 13 (1957).

<sup>7</sup> Palevsky, Otnes, Larsson, Pauli, and Stedman, Phys. Rev. **108**, 1346 (1957).

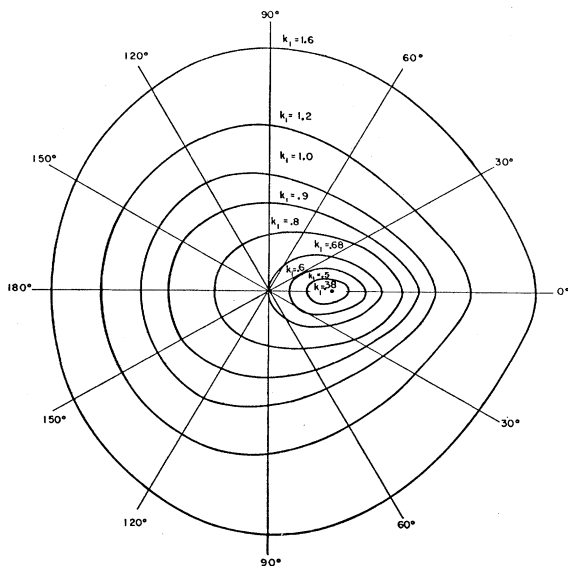


FIG. 1. Scattering surfaces for neutrons losing energy to helium II. Each curve is labeled with the wave number of the incident neutrons. The momentum ( $p = \hbar k$ ) of the scattered neutrons for any scattering angle  $\theta$  is measured by the length of the line drawn from the origin to the curve of the particular incident momentum.

The neutron kinematics are perhaps best visualized by plotting the solution of Eqs. (1) and (2) for a particular dispersion relation  $E(\kappa)$ . Cohen and Feynman<sup>6</sup> chose the Landau dispersion relation with  $c = 240$  m/sec,  $\Delta = 9.6^\circ\text{K}$ ,  $p_0/\hbar = 1.95 \text{ \AA}^{-1}$ ,  $\mu = 1.06 m_{\text{He}}$ . The solutions of the equations plotted as a family of curves for different incident neutron wave number is shown in Fig. 1. The wave numbers,  $k_0$ , of the incident neutrons are shown along the  $\theta = 90^\circ$  axis. For a given incident neutron momentum ( $p = \hbar k$ ) the energy of the scattered neutron for any scattering angle  $\theta$  (measured with respect to the incident neutron direction) is measured by the length of a line drawn from the origin, at an angle  $\theta$ , to the curve of the particular incident momentum. In general for a fixed incoming neutron momentum the excitation momentum ( $\kappa$ ) increases with increasing angle of scattering. For a fixed angle between the incident and scattered neutron,  $\kappa$  increases with increasing incident neutron momentum. The measurement of  $E$  as a function of  $\kappa$  can be carried out by using a fixed incident energy and varying the angle between incident and scattered neutrons or by keeping the scattering angle fixed and varying the incident neutron energy. Both methods were utilized in the experiment reported in this paper.

One can also estimate from Fig. 1 the experimental conditions necessary to investigate a certain portion of the assumed dispersion curve. For example, to investigate the region of the roton minimum the length of the vector between incident and scattered neutrons must correspond to  $p/\hbar = 1.95 \text{ \AA}^{-1}$ . For  $1.6 \text{ \AA}^{-1}$  incident neutrons this geometrical construction gives a scattering

angle of approximately  $80^\circ$ . It is also clear that for neutrons of momentum less than  $1.15 \text{ \AA}^{-1}$  one cannot excite a roton of minimum energy (assuming that the dispersion relation used is correct). If a roton of minimum energy is excited by a  $1.6 \text{ \AA}^{-1}$  incident neutron, the momentum of the scattered neutron is  $1.4 \text{ \AA}^{-1}$ . The minimum roton energy corresponds to a temperature of  $10^\circ\text{K}$ . Therefore, in order to measure this energy to  $\pm 1^\circ\text{K}$  requires that the incoming and outgoing momentum be defined to approximately 1%.

To perform the experiment in the most straightforward manner, using a monochromator in the incident neutron beam and analyzing the scattered beam with a spectrometer, was impossible with the neutron flux available at the Stockholm reactor. To overcome the problem of low neutron intensity a method was used which defined certain energies of a thermal neutron spectrum with very little loss of neutron intensity. If a thick sample (filter) of a polycrystalline material is placed in a neutron beam emerging from a reactor, then nearly all of the neutrons with wavelength shorter than twice the separation of the most widely spaced planes in the crystal are scattered out of the beam by Bragg scattering. For longer wavelengths, the material becomes transparent for neutrons, provided the nuclear absorption and incoherent scattering of the filtering material is small. The intensity of the filtered beam rises discontinuously at the "Bragg cutoff" wavelength and then follows the shape of the reactor spectrum as illustrated in Fig. 2. In practice the sharpness of the rise of intensity at the Bragg cutoff is determined by

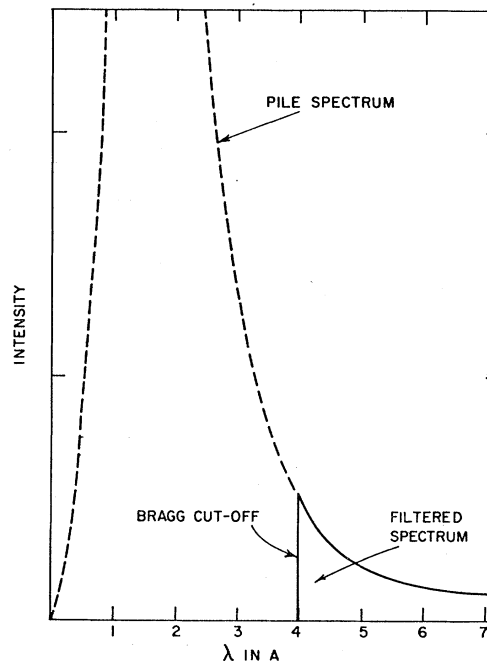


FIG. 2. Thermal neutron spectrum of pile neutrons. The heavy solid line indicates the portion of the spectrum that passes through beryllium with little attenuation.

the resolution of the spectrometer used to measure the rise. Under favorable experimental conditions it is possible to define the position of the Bragg cutoff to about 10% of the resolution width. When such a filtered spectrum is incident upon the helium sample the spectrum observed at some fixed angle  $\theta$  is expected to resemble the shape of the incident spectrum but be shifted to lower energies. The sharpness of cutoff observed in the scattered beam will depend on the resolution of the neutron spectrometer and on the mean free path of the excitations produced in helium. Finally the experiments require good filters possessing cutoff wavelengths in the region of interest for investigating the excitations in He II. Fortunately Be, which is about the best filter material available, has a Bragg cutoff at  $\lambda = 3.95 \text{ \AA}$ ,  $k = 1.58 \text{ \AA}^{-1}$ . As was shown above when neutrons of this wavelength are incident on He II, the interaction to produce rotons in the region of minimum energy scatters the neutron through approximately  $90^\circ$ . A spectrometer of 3% velocity resolution was used in the experiment and therefore it was expected that  $\Delta$  could be measured to about  $\pm 0.3^\circ\text{K}$ .

### III. EXPERIMENTAL APPARATUS

The experimental equipment used to measure the excitation spectrum in He II consists of three parts:

1. Neutron energy monochromator: a Be filter cooled to liquid nitrogen temperature giving a neutron spectrum with a sharp cutoff at  $3.95 \text{ \AA}$ , or a BeO filter giving a cutoff at  $4.68 \text{ \AA}$ .

2. A helium cryostat constructed to contain about 1.5 liters of liquid helium with a pumping system allowing a reduction of the pressure above the free helium to 2.5 mm corresponding to a temperature of  $1.4^\circ\text{K}$ .

3. Neutron energy analyzer: a slow-chopper time-of-flight spectrometer, the chopper and detector being mounted on an arm, which can be rotated around the cryostat axis in a vertical plane. A one-hundred channel time analyzer sorts out the detector pulses according to neutron flight time.

#### A. Spectrometer Arrangement

The filter and chopper mentioned under 1 and 3 above are mounted in front of one of the experimental channels of the Stockholm heavy water reactor as schematically shown in Fig. 3. The essential parts of the equipment, i.e., the filter, the chopper, and the detector have been described elsewhere.<sup>8</sup> Only those details which have a direct bearing on this experiment will be given here.

The reactor is operated at 600 kw giving a maximum central flux of  $10^{12} \text{ n/cm}^2 \text{ sec}$  and a thermal flux of  $\sim 3.5 \times 10^8 \text{ n/cm}^2 \text{ sec}$  emerging from the beam channel at the face of the reactor shield. The full angular spread of the neutron beam is  $4.5^\circ$ . A filter of poly-

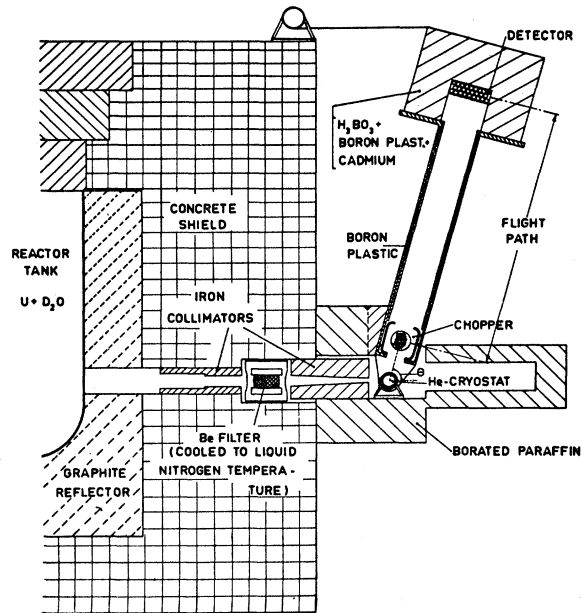


FIG. 3. Schematic diagram of apparatus used to perform helium experiment.

crystalline beryllium 20 cm thick is placed in the channel, and the neutron beam is defined by a thick inner collimator and a conical outer collimator with a rectangular opening of maximum dimensions  $5 \times 10 \text{ cm}^2$ .

On a rigid steel framework in front of the exit collimator, heavy shielding consisting of about 40 cm of borated paraffin and boron carbide is placed in order to keep stray neutrons from leaving the reactor shield. The same framework also holds the bearings for a 350-cm long rigid arm, which can be rotated in the vertical plane. At the place where the horizontal central plane of the beam—corresponding to maximum intensity—and the arm axis intersect there is ample space for placing samples such that the sample axis coincides with the axis of rotation of the arm. On this arm above the sample is mounted the slow chopper, with its axis of rotation aligned parallel to the sample axis. The distance between the chopper axis and sample axis is 35 cm. Beyond the chopper follows a three meters long neutron flight path, completely shielded by a tube of rectangular section of dimensions  $20 \times 30 \text{ cm}^2$ , the shielding material consisting of 1-cm thick boron plastic. The full opening angle for the neutrons leaving the chopper is  $4.5^\circ$ , the same as the angular spread of the beam entering the sample cryostat. On top of the shielding tube is mounted the detector consisting of  $29 \text{ B}^{10}\text{F}_3$  proportional counters with a sensitive area of  $20 \times 30 \text{ cm}^2$  and a depth of 8 cm. The detector is surrounded by a shielding box of minimum thickness 30 cm, terminating the arm. The shielding material in the box is boric acid and thick layers of boron plastic and cadmium. Thus the entire flight path is completely shielded against thermal neutrons and very effectively

<sup>8</sup> Larsson, Stedman, and Palevsky, *J. Nuclear Energy* 6, 222 (1958).

against fast neutrons. To further reduce background a 2.5 meters deep cylindrical beam catcher made of borated paraffin of 10 cm thickness intercepts the incident neutron beam after it passes through the sample. The  $\text{BF}_3$  counter bank is designed to stop approximately 75% of the scattered neutrons, yielding the maximum counting rate consistent with a good ratio of real to background counts. The detector pulses are sorted according to neutron time of flight in a 100-channel time analyzer of variable channel width from 2–100  $\mu\text{sec}$ .

### B. Time Resolution

The chopper, which has curved slits to give a rather flat transmission function, gives a burst length of 30  $\mu\text{sec}$  at a speed of rotation of 13 000 rpm. The counting channel width normally used in these experiments was also 30  $\mu\text{sec}$ . The total resolution of the spectrometer system is determined experimentally using the beryllium break at 3.95 Å. This break and the graphite break at 6.70 Å were also used to calibrate the time scale when the chopper was first put into operation. In addition to the above time uncertainties, the resolution includes a contribution from the uncertainty in neutron flight path resulting from the detector thickness and small contributions from the finite angular spreads of the incident and detected neutrons. The resolution function is symmetrical and for the purpose of calculations may be approximated by either a Gaussian or a triangular function. From a study of the shape of the cutoff spectrum (see Fig. 6), one can deduce that the full width at the half maximum of the resolution function is approximately 100  $\mu\text{sec}$ . The time of flight of the scattered neutrons is approximately 3000  $\mu\text{sec}$ . As was shown in Sec. II, in order to measure  $\Delta v$  to  $\pm 1^\circ\text{K}$ , the uncertainty in incident and scattered neutron momenta must be  $\pm 1\%$ , or 30  $\mu\text{sec}$  in time of flight. More correctly stated, the *difference in positions* of the cutoffs in the incident and scattered beams must be determined to 30  $\mu\text{sec}$ . Provided the shape of the Bragg cutoff does not change in the scattering process, any point on the sharp rise at the cutoff may be used to measure this difference. However, the point midway between the minimum and maximum counting rates is chosen because this point is insensitive to small changes in the shape of the spectrum. For example, for the neutron spectrum obtained from the reactor and the resolution width of 100  $\mu\text{sec}$  one can calculate that the midpoint is separated by less than 3  $\mu\text{sec}$  from the position where the Bragg cutoff would have been observed with infinite resolution.

In order to obtain an experimental check on how well the position of the Bragg cutoff could be measured with the above apparatus, the Be cutoff was measured for a number of different settings of the analyzer. Data were taken over a period of several days with various channel widths and time decay settings. For five

different sets of data, the maximum deviation of the cutoff position was found to be 10  $\mu\text{sec}$ . On the basis of these first tests it was concluded that with good counting statistics the separation of the cutoffs could readily be defined to  $\pm 15 \mu\text{sec}$ .

### C. Helium Cryostat

A sketch of the liquid helium cryostat is shown in Fig. 4 which also gives the dimensions. It is all-metal construction consisting of a liquid helium scattering chamber, a liquid helium storage vessel, radiation shields, and a liquid nitrogen storage vessel mounted in a vacuum jacket made of aluminum. All the internal structures are suspended from a brass top plate of the vacuum jacket by five stainless steel tubes. Four of these have a 10-mm outer diameter and a wall thickness of 0.15 mm and are mounted equally spaced around a circle. They extend through the top plate and are used for filling the liquid nitrogen vessel and for exhausting the nitrogen vapor. The central helium filling tube is 30 mm in diameter with a wall thickness of 0.35 mm.

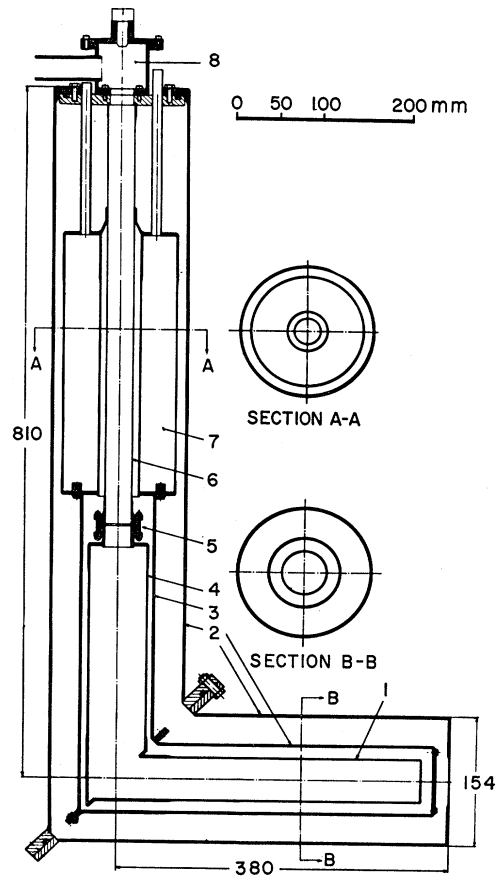


FIG. 4. Schematic diagram of helium cryostat for neutron measurements. (1) Aluminum-walled helium container; (2) vacuum chamber; (3) radiation shield; (4) helium reservoir; (5) aluminum to stainless steel knife-edge joint; (6) stainless steel filling cylinder; (7) liquid nitrogen reservoir; (8) central helium filling tube.

It is soft-soldered to the top plate of the vacuum jacket. The liquid nitrogen vessel is made of copper and holds about 3 liters. Good contact between the nitrogen vessel and the central tube is achieved by soft-soldering. A radiation shield, in which the vertical and the horizontal sections are made of copper and aluminum, respectively, is attached to the bottom of the liquid nitrogen vessel by means of screws. Thermal contact between the two sections is achieved by a flange joint. The copper structures are chromium-plated in order to get a low coefficient of emissivity.

The liquid helium scattering chamber and the storage vessel are made of aluminum and contain together about 1.5 liters. Aluminum is used to keep the intensity of neutrons scattered by the container at a minimum. The storage vessel is connected to the central stainless steel tube by a screw joint. A V-shaped edge of steel is pressed into an aluminum plate, thus making the vacuum seal. A header is sealed to the top plate of the vacuum jacket by O-ring gaskets. In the top of the header is a hole with two O-rings providing airtight seal for the transfer tube. To the header are connected an exhausting tube and a calibrated vacuum dial gauge of capsule type, barometrically compensated, with a range of 0–20 mm Hg. By reducing the pressure over the surface the temperature of the liquid helium can be lowered. This was done with a one-stage 450-liter/min rotary pump. The lowest pressure obtained was 2.4 mm Hg corresponding to a temperature of 1.42°K.

The helium system is closed and the evaporated helium gas is recovered in 1200-liter rubber balloons. Before filling with liquid helium the cryostat vacuum jacket is evacuated to a pressure of about  $5 \times 10^{-6}$  mm Hg. All the air in the helium system is pumped out and helium gas is let in. Then the liquid nitrogen storage vessel is filled. It requires about 5 hours and 4 liters of liquid nitrogen to establish equilibrium temperatures in the radiation shield. The equilibrium loss rate of liquid nitrogen is about 250 ml/hour. Liquid helium is then transferred through a siphon from a Dewar to the cryostat. The progress of filling is followed with carbon resistors, one at the bottom and one at the top of the helium cryostat storage vessel. It requires about 2 liters to cool the scattering chamber and the storage vessel from liquid nitrogen to liquid helium temperature, after which the loss rate is 100 ml/hour.

#### IV. MEASUREMENTS

##### A. The Scattering of Cold Neutrons from Liquid He Above and Below the $\lambda$ Point

For the first measurements the apparatus was arranged so that the angle between the direction of the incident and scattered neutrons was fixed at 90°. With the sample cryostat evacuated, data were taken (1) to check the intensity of “background” neutron, coming from all sources other than the helium, and (2) to ascertain if structure could be observed in the back-

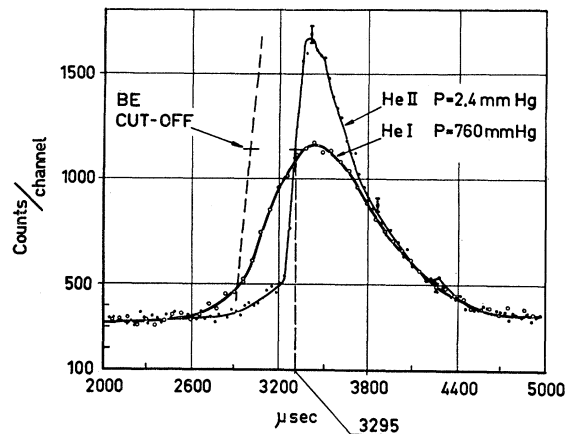


Fig. 5. Spectrum of neutrons scattered by helium. The ordinate gives the number of counts accumulated in a 30- $\mu$ sec interval at the time of flight indicated on the abscissa. The light solid line represents the scattered neutron from He at 1.4°K, the heavy solid line from He at 4.2°K. The dashed line gives the position of the Be cutoff in the incident spectrum.

ground that might distort the spectrum of helium-scattered neutrons. The background was found to be constant (independent of neutron energy) and amounted to approximately 10% of the intensity observed from the helium sample. Next the cryostat was filled with helium and pumped to a pressure of 2.4 mm corresponding to a temperature of 1.4°K and data were taken for approximately 3 hours. These data are indicated by the light solid line of Fig. 5. The scattered spectrum exhibits the same sharp rise characteristic of the Be cutoff in the incident spectrum (dashed line); however, the position of the cutoff is displaced some 305  $\mu$ sec towards greater time of flight (lower energy). This was the first direct experimental evidence that excitations with long mean free paths compared to their wavelength exist in He II. Next the cryostat was filled with helium at atmospheric pressure, and data were again accumulated for 3 hours. The results are shown as the heavy solid line in Fig. 5. The spectrum no longer exhibits the sharp cutoff character. The broad nature of the spectrum indicates that there are many-collision processes present, and qualitatively the spectrum has the shape one would expect from a normal fluid. It is interesting to note that the integral over neutron energy of the scattered intensity is approximately the same below and above the  $\lambda$  point. It is for this reason that Sommers, Dash, and Goldstein<sup>9</sup> could not observe any sharp change in total cross section as the helium passed through the  $\lambda$  point.

##### B. Dispersion Curve in the Momentum Region $1.50 \leq \kappa \leq 2.14 \text{ \AA}^{-1}$

Having established that nature of the excitations in He II is consistent with the theories presented by Landau and Feynman, the next experimental step was

<sup>9</sup> Sommers, Dash, and Goldstein, Phys. Rev. **97**, 855 (1955).

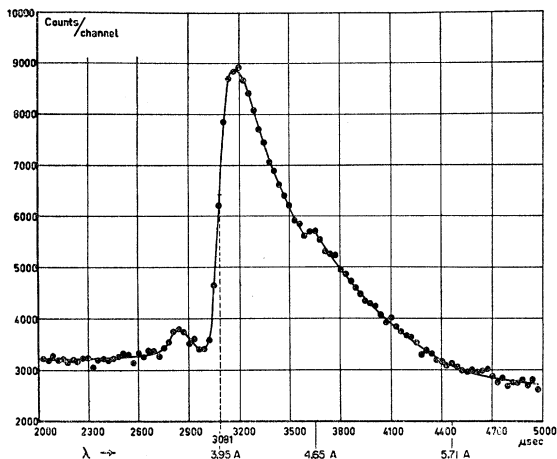


FIG. 6. The spectrum of beryllium-filtered neutrons as observed by scattering from vanadium. The position of the break is found to be independent of the scattering angle and corresponds to a cutoff wavelength of 3.95 Å.

to determine the energy of the excitations as a function of their momentum (dispersion curve). The region of the roton minimum is of greatest interest both from the theoretical and experimental point of view. Measurements were therefore made to locate the minimum and measure the energy ( $\Delta$ ) at this point.

The difference in position of the cutoff observed in the scattered spectrum as compared to the incident spectrum is a direct measure of the energy of the excitation produced by the neutron [see Eq. (3)]. In order to measure this difference with the least possible systematic error, the incident spectrum was measured under exactly the same experimental conditions as the scattered-neutron spectrum. This was done by substituting a thin vanadium sample in place of the helium sample. The scattering amplitude of vanadium is nearly totally incoherent and for low-energy Be-filtered neutrons the scattering is essentially elastic. Therefore the vanadium sample acts to scatter the incident beam isotropically and with no change in energy, with the result that incident spectrum can be measured at any angle of scattering, with the same angular definition as was used to measure the helium-scattered neutrons. Measuring the incident spectrum in this way gave the first point on the dispersion curve at a wave number  $\kappa = 2.14 \pm 0.07 \text{ \AA}^{-1}$  ( $\kappa = 2\pi/\lambda$ ) and energy  $E = 10.7 \pm 0.5^\circ \text{K}$ .

In order to measure a series of different excitations energies, two experimental methods are available as explained in Sec. II. These are (1) to vary the incoming neutron energy by using different filters such as Be, BeO, Pb, graphite, keeping the angle of scattering fixed, and (2) to use one filter to define the incoming neutron energy and vary the angle of observation of the scattered neutrons.

An inspection of the spectrum transmitted by the beryllium filter (Fig. 6) shows that the use of a BeO

filter with the last Bragg cutoff at 4.68 Å cuts the intensity of cold neutrons down by a factor of two. The situation would be much worse using a Pb filter with the cutoff at 5.71 Å and graphite with a cutoff wavelength of 6.70 Å. The use of filters other than Be and possibly BeO were thus prohibited by the relatively low intensity delivered by the Stockholm reactor. This conclusion led to the construction of the arm arrangement described in Sec. III above. In this arrangement the He cryostat is put into the beam in such a way that the cryostat axis of symmetry coincides with the axis of rotation of the arm.

The procedure followed in the experiment was as follows: The arm was set at a certain angle,  $\theta$ , and a few runs were taken with the cryostat filled with liquid helium. The pressure in the cryostat was varying somewhat between 2.5 and 3.2 mm Hg corresponding to helium temperatures of 1.4–1.5°K. Each run was repeated until a number of counts corresponding to a statistical error of about 3% or better were accumulated in the peak. This as a rule involved three to five runs of three hours each. The standard running conditions were at a chopper speed of 13 000 rpm and an electronic channel width of 30  $\mu\text{sec}$  corresponding to a resolution width of 100  $\mu\text{sec}$ . To make sure that the time calibration remained constant, the helium cryostat was removed between some of the runs and a vanadium sample was placed in the beam. The time position of the beryllium break was found to be independent of angular setting within  $\pm 5 \mu\text{sec}$  and the average position of the break was found to be  $(3081 \pm 5) \mu\text{sec}$  in exact agreement with the time position calculated from the known flight path (see Fig. 6). Background runs were also taken at different angular settings with the empty cryostat in the beam. This background was found to be constant and independent of time and angular setting.

Following this scheme two sets of runs were taken at 90°, one with the Be filter and another with a 10-cm BeO filter added. The scattered intensity when using the BeO filter was so low that no more runs were taken with the BeO filter. Using the Be filter, eight more sets of runs were taken for angular settings of 86.0°,

TABLE I. Helium scattering data for  $T = 1.4\text{--}1.5^\circ \text{K}$ .

Filter used	Angle of observation $\theta^\circ$	Time of flight for		Time shift of break position $\Delta t = t_0 - t_f$ ( $\mu\text{sec}$ )
		ingoing neutrons $t_0$ ( $\mu\text{sec}$ )	scattered neutrons $t_f$ ( $\mu\text{sec}$ )	
Be	59.4	3081 $\pm$ 5	3415 $\pm$ 10	334 $\pm$ 11
Be	63.6	3081 $\pm$ 5	3395 $\pm$ 10	314 $\pm$ 11
Be	67.7	3081 $\pm$ 5	3347 $\pm$ 10	266 $\pm$ 11
Be	69.6	3081 $\pm$ 5	3338 $\pm$ 10	257 $\pm$ 11
BeO	90.0	3524 $\pm$ 10	3917 $\pm$ 15	393 $\pm$ 18
Be	76.3	3081 $\pm$ 5	3305 $\pm$ 10	224 $\pm$ 11
Be	80.2	3081 $\pm$ 5	3317 $\pm$ 10	236 $\pm$ 11
Be	83.0	3146 $\pm$ 10	3392 $\pm$ 10	246 $\pm$ 15
Be	86.0	3081 $\pm$ 5	3362 $\pm$ 10	281 $\pm$ 11
Be	90.0	2992 $\pm$ 5	3297 $\pm$ 10	305 $\pm$ 11

83.0°, 80.2°, 76.3°, 69.6°, 67.7°, 63.6°, and 59.4°. One set of data at 86.0° was taken with the sample at  $T=1.75^\circ\text{K}$ . The scattered neutron intensity gradually decreased with decreasing angles and at the last angle of 59.4° 15 hours running time was necessary to get 1000 counts in the scattered peak of which 500 counts correspond to background neutrons. Defining the positions of the incident and scattered beryllium breaks as described in Sec. IIIB, we arrive at the results for the flight times given in Table I. The time shift of the break, corresponding to the energy necessary to excite a roton, is given for each angular setting. The errors given as associated with each break definition are estimated from the statistics of the run and by an analysis of the possible extreme positions for each break. As seen from the table, the time shifts are more than ten times smaller than the flight times themselves, which means that high resolution is necessary to define the shifts to good accuracy. Examples of the spectra scattered from He II at various sample temperatures are given in Figs. 7 (A), (B), and (C).

At  $T=1.42^\circ\text{K}$  the spectrum of scattered neutrons has the same shape as the incident spectrum (Fig. 6). The small maximum in counting rate at approximately  $t=3000 \mu\text{sec}$  is a result of incomplete filtering action by the Be filter and is also observed in the incident beam. Figures 7 (B) and (C) show the change in shape

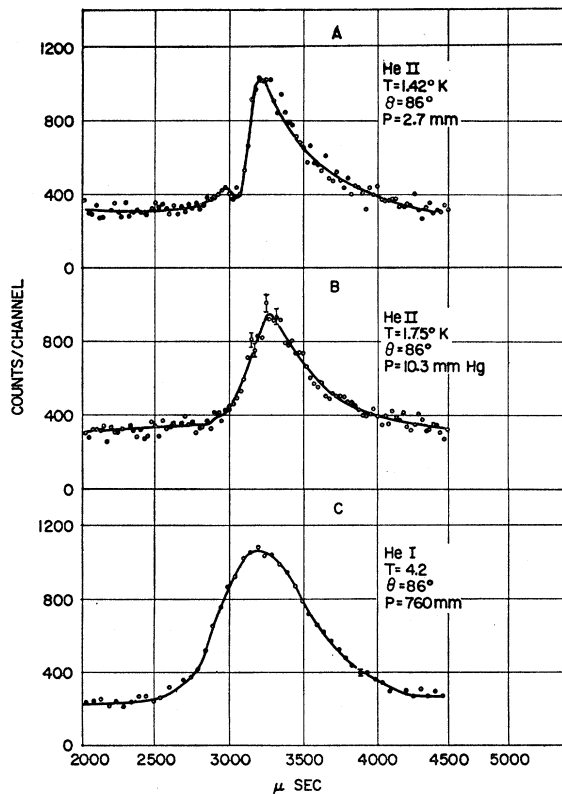


FIG. 7. Examples of spectra of neutrons scattered from liquid helium at various sample temperatures.

TABLE II. Dispersion relation for excitations in He II.  $T=1.4-1.5^\circ\text{K}$ .

Angular setting $\theta$	$\kappa \text{ \AA}^{-1}$	$E^\circ\text{K}$
59.4	$1.50 \pm 0.05$	$11.3 \pm 0.4$
63.6	$1.60 \pm 0.05$	$10.8 \pm 0.4$
67.7	$1.70 \pm 0.05$	$9.3 \pm 0.4$
69.6	$1.75 \pm 0.05$	$9.0 \pm 0.4$
90.0	$1.81 \pm 0.05$	$8.3 \pm 0.6$
76.3	$1.90 \pm 0.04$	$8.0 \pm 0.4$
80.2	$1.98 \pm 0.04$	$8.4 \pm 0.4$
83.0	$2.03 \pm 0.04$	$8.5 \pm 0.5$
86.0	$2.08 \pm 0.05$	$9.8 \pm 0.4$
90.0	$2.14 \pm 0.05$	$10.7 \pm 0.4$

of the scattered spectrum with increasing temperature. As the break broadens, its center also changes, moving towards the position of the Be cutoff.

### C. Calculation of $\kappa$ and $E$ Accuracy

The Eqs. (1) and (2) of Sec. II may be rewritten to include experimentally determined quantities,

$$E(^{\circ}\text{K}) = \frac{\hbar^2}{2mk_B\lambda_c^2} \left( \frac{t_0 + t_f}{t_f^2} \right) \Delta t, \quad (3)$$

$$\kappa = \frac{2\pi (t_0^2 + t_f^2 - 2t_0t_f \cos\theta)^{\frac{1}{2}}}{\lambda_c t_f}, \quad (4)$$

where  $m$  is the neutron mass;  $k_B$  is the Boltzmann constant;  $\lambda_c$  is the cutoff wavelength for the filter used, 3.952 Å for the Be filter and 4.677 Å for the BeO filter;  $\theta$ ,  $t_0$ ,  $t_f$ , and  $\Delta t$  being defined in Table I. In this formulation it is also easily seen that the error in the determination of the energy is almost completely determined by the error in  $\Delta t$ , the total errors in  $E$  emanating from all other sources being of the order of 0.5% (compare Table I). In a similar way the main contribution to error in  $\kappa$  comes from the uncertainty in the angular definition,  $\pm d\theta$ , because errors due to uncertainties in  $t_0$  and  $t_f$  are small. Two effects have to be considered in discussing the angular definition. First, the angular setting of the arm with respect to the incoming neutron beam is accurate to  $\pm 0.5^\circ$ . Secondly, a systematic error might arise in the angular definition because of the relatively large angular openings,  $\pm 2.3^\circ$  each, of the incoming and outgoing beams. If the differential cross section for the scattering process varies rapidly over an angle of the order of the acceptance angle, i.e.,  $4.5^\circ$ , most of the intensity recorded might originate from one extreme side of the beam hole and one extreme side of the detector. However, a calculation of the differential scattering cross section using the formulas of Cohen and Feynman shows that the variation of the scattered intensity over the detector acceptance angle can at most lead to an error of  $\pm 1^\circ$  in the angular definition. (The uncertainty in energy resulting from the angular uncertainty is negligible compared to the error in  $\Delta t$ .)

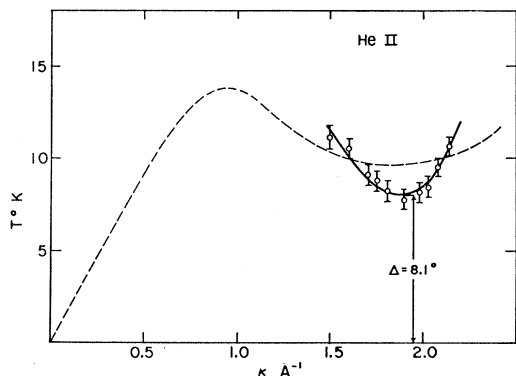


FIG. 8. Dispersion curve for excitations in He II. The temperature of the sample was kept between 1.4 and 1.5°K. The dashed line is the Landau-Feynman dispersion curve given in reference 6.

Using these considerations the final results ( $\kappa_i, E_i$ ) defining the dispersion relation are as given in Table II.

### V. RESULTS AND DISCUSSION

Figure 8 shows a plot of the data given in Table II. A least-squares fit to these data using a parabola of the Landau type,  $E = \Delta + (p - p_0)^2/2\mu$ , in the region  $\kappa = 1.7 - 2.1 \text{ \AA}^{-1}$  agrees with the data within the limits of experimental error. The derived constants are

$$\begin{aligned}\Delta &= 8.1 \pm 0.4^\circ\text{K}, \\ p_0/\hbar &= 1.90 \pm 0.03 \text{ \AA}^{-1}, \\ \mu &= 0.16 \pm 0.02 m_{\text{He}}.\end{aligned}$$

As can be seen from Fig. 8, the experimental dispersion curve is not really parabolic. However, the above constants can be compared to those derived from specific heat and second sound data at low temperatures because in such measurements only rotons near the minimum of the dispersion curve are excited. The values obtained from recent "low-temperature integral" experiments give somewhat conflicting results. Khalatnikov<sup>10</sup> in 1952 gave  $\Delta = 8.9 \pm 0.2^\circ\text{K}$ ,  $p_0/\hbar = 2.0 \pm 0.05 \text{ \AA}^{-1}$ ,  $\mu = 0.32 \pm 0.13 m_{\text{He}}$  whereas de Klerk, Hudson, and Pellam<sup>11</sup> quote  $\Delta = 9.6^\circ\text{K}$ ,  $p_0/\hbar = 2.30 \text{ \AA}^{-1}$ ,  $\mu = 0.40 m_{\text{He}}$ , and Kramers<sup>12</sup> quotes  $\Delta = 9.0 \pm 0.2^\circ\text{K}$ ,  $p_0/\hbar = 2.0 \pm 0.1 \text{ \AA}^{-1}$ ,  $\mu = 0.3 \pm 0.15 m_{\text{He}}$ .

The largest discrepancy between the neutron data and the integral measurements appears to be in the value of  $\Delta$ , the neutron value being some 10% lower than the value quoted by Khalatnikov and Kramers and 15% lower than the value quoted by de Klerk *et al.*

In light of the neutron measurements it seems clear that the wave function used by Feynman and Cohen<sup>13</sup>

to describe the roton needs to be modified. On the basis of the Feynman theory, relating the dispersion curve for helium excitations to the differential x-ray scattering cross section of helium, the values of the Landau parameters are  $\Delta \leq 11.5^\circ\text{K}$ ,  $p_0/\hbar = 1.85 \text{ \AA}^{-1}$ ,  $\mu \approx 0.20 m_{\text{He}}$ . A recent attempt by Brueckner and Sawada<sup>14</sup> to find the dispersion relation for a dense Bose-Einstein hard-sphere gas yields a formula which qualitatively gives the correct shape of the dispersion curve, *viz.*, starting with a linear rise, reaching a maximum, and then exhibiting the roton minimum. The theory contains two adjustable parameters, the fluid density and the distance of closest approach of two helium atoms. If these parameters are adjusted to give the values of  $\Delta$  and  $p_0/\hbar$  obtained from the neutron data, the computed velocity of sound is some 20% greater than the measured value. If the velocity of sound and  $\Delta$  are assigned, the theoretical value of  $p_0/\hbar$  is found to be 30% low.

By using the uncertainty principle  $\Delta p \Delta x = \hbar$  and the criterion that a change in the spread of the break of 15  $\mu\text{sec}$  or greater would be experimentally observable, the data taken at  $T = 1.42^\circ\text{K}$  [Fig. 7(A)] indicate that the mean free path of a roton is equal or greater than sixty times its wavelength ( $\Delta X \geq 10^{-6} \text{ cm}$ ). This figure may be compared to a value of  $\Delta X \leq 2 \times 10^{-6} \text{ cm}$  as calculated from the Landau-Khalatnikov<sup>15</sup> theory. The observed spreading of the break at  $T = 1.75^\circ\text{K}$  [Fig. 7(B)] is consistent with a roton mean free path of only six times its wavelength. It is interesting to note that although the mean free path of this  $2.08 \text{ \AA}^{-1}$  roton is reduced by a factor of 10 in going from  $T = 1.42^\circ\text{K}$  to  $T = 1.75^\circ\text{K}$ , the energy of the roton changes only by  $-0.5 \pm 0.5^\circ\text{K}$ . One therefore would expect that  $\Delta$  in first order would be independent of temperature over the temperature interval 0–1.7°K. For temperatures greater between 1.7° and 4.2°K the interaction between excitations causes a rapid washing out of the sharp character of the break in the scattered neutron spectrum [Fig. 7(C)] and the portion of the break moves in such a way as to decrease the computed value of  $\Delta$ .

### ACKNOWLEDGMENTS

The authors wish to thank Dr. R. Pauli and Mr. R. Stedman for their aid in making the first measurements. We are indebted to Professor J. O. Linde and Mr. K. Svensson of KTH in Stockholm for their aid with the cryogenics of the experiment, and to Dr. M. Cohen, Professor R. P. Feynman, and Professor L. van Hove for many enlightening discussions concerning the nature of helium II. One of us (Harry Palevsky) is indebted to Dr. S. Eklund and the Swedish Atomic Energy Commission for his very enjoyable stay in Sweden.

<sup>10</sup> E. M. Khalatnikov, J. Exptl. Theoret. Phys. (U.S.S.R.) **23**, 21 (1952).

<sup>11</sup> de Klerk, Hudson, and Pellam, Phys. Rev. **93**, 28 (1954).

<sup>12</sup> H. C. Kramers, thesis, Leiden, 1955 (unpublished).

<sup>13</sup> R. P. Feynman and M. Cohen, Phys. Rev. **102**, 1189 (1956).

<sup>14</sup> K. A. Brueckner and K. Sawada, Phys. Rev. **106**, 1128 (1957).

<sup>15</sup> L. Landau and I. Khalatnikov, J. Exptl. Theoret. Phys. (U.S.S.R.) **19**, 637, 709 (1949).